AD-A069 276 FAIRCHILD REPUBLIC CO FARMINGDALE N Y F/G 21/8
ELECTRODE EROSION PROCESSES IN PULSED PLASMA THRUSTERS.(U)
MAR 79 D J PALUMBO, M BEGUN, W J GUMAN F04611-77-C-0024
UNCLASSIFIED MS181R0001 AFRPL-TR-79-14 NL

| OF |
AD
A069276

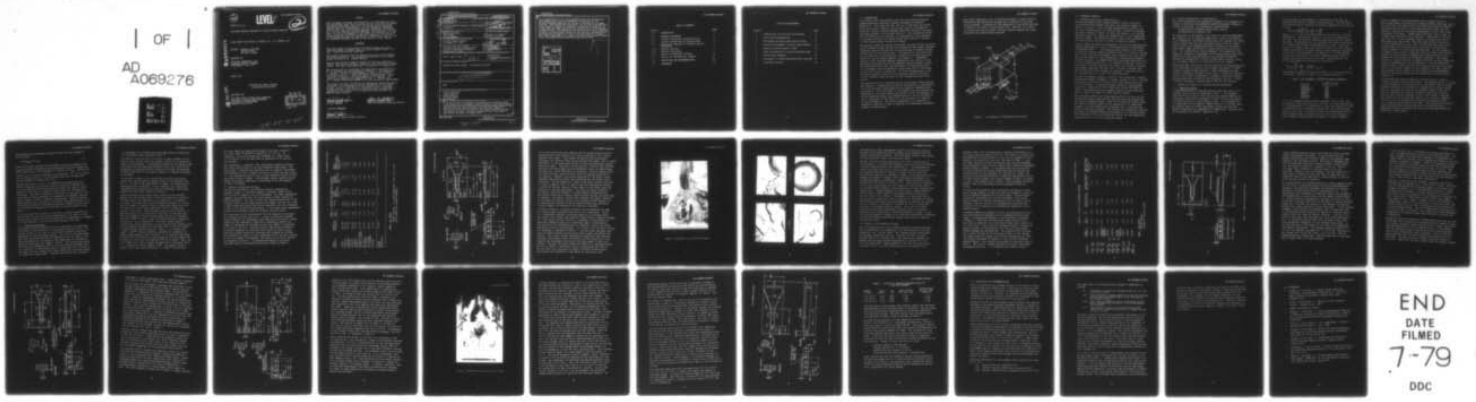

END
DATE
FILMED
7-79
DDC

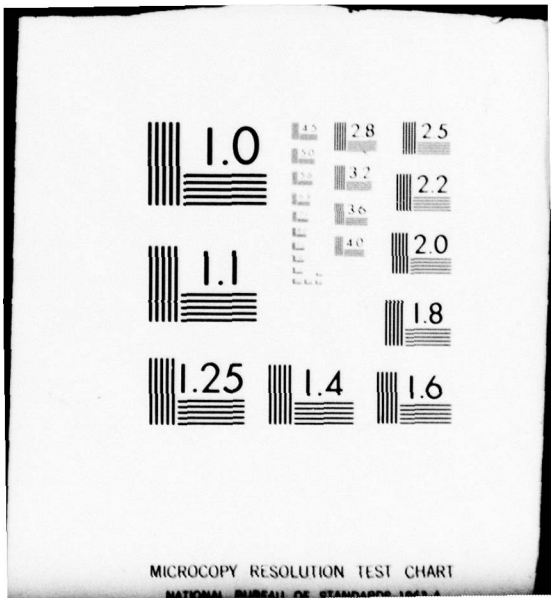
1.0
1.1
1.25
1.4
1.6
1.8
2.0
2.2
2.5
2.8
3.2
3.6
4.0
MICROCOPY RESOLUTION TEST CHART

LEVEL II

FRC DOCUMENT MS181R0001

2

B. S.

AFRPL-TR-79-14

ELECTRODE EROSION PROCESSES IN PULSED PLASMA THRUSTERS

FINAL REPORT FOR PERIOD 15 AUGUST 1977 - 31 JANUARY 1979

AUTHORS: DOMINIC J PALUMBO
MARTIN BEGUN
WILLIAM J GUMAN

PREPARED BY:

FAIRCHILD INDUSTRIES, INC
FAIRCHILD REPUBLIC COMPANY
FARMINGDALE LI NY 11735

MARCH 1979

APPROVED FOR PUBLIC RELEASE
DISTRIBUTION UNLIMITED

PREPARED FOR:

AIR FORCE ROCKET PROPULSION LABORATORY
DIRECTOR OF SCIENCE AND TECHNOLOGY
AIR FORCE SYSTEMS COMMAND
EDWARDS AFB CA 93523

79-05 21 051

NOTICE

When Government drawings, specifications, or other data are used for any purpose other than in connection with a definitely related Government procurement operation, the United States Government thereby incurs no responsibility nor any obligation whatsoever; and the fact that the Government may have formulated, furnished, or in any way supplied the said drawings, specifications, or other data, is not to be regarded by implication or otherwise as in any manner licensing the holder or any other person or corporation, or conveying any rights or permission to manufacture, use, or sell any patented invention that may in any way be related thereto.

FOREWORD

This final report was prepared by Fairchild Industries, Inc., Fairchild Republic Company under Air Force Contract F04611-77-C-0024, "Electrode Erosion Processes".

The research reported upon was supported by the Air Force Rocket Propulsion Laboratory. The program was monitored in the Liquid Rocket Division by Lt. Michael Brasher.

Work on this contract began in August 1977 and was completed in January 1979 and the pertinent studies of this period are reported herein. The report was submitted by the Authors in January 1979.

The authors wish to acknowledge the significant contributions of Mr. M. Katchmar and the assistance of Messrs. S. Pasternack and F. Carlson. Specific acknowledgement is made to the valuable contributions of Dr. J. Perel of Phrasor Technology who, as sub-contractor, assisted in the development of the Analyses. The constructive comments and suggestions of Mr. J. Bechdol and Mr. G. Unrah of Fairchild Republic are also gratefully acknowledged.

This report has been reviewed by the Information Office/XOJ and is releasable to the National Technical Information Service (NTIS). At NTIS it will be available to the general public, including foreign nations. This technical report has been reviewed and is approved for publication; it is unclassified and suitable for general public release.

Michael R. Brasher
MICHAEL BRASHER, 1LT
Project Manager

Thomas W. Waddell
THOMAS W. WADDELL, Chief
High Performance Propulsion Section

FOR THE COMMANDER

Edward E. Stein
EDWARD E. STEIN,
Deputy Chief, Liquid Rocket Division

UNCLASSIFIED

SECURITY CLASSIFICATION OF THIS PAGE (When Data Entered)

(19) REPORT DOCUMENTATION PAGE

READ INSTRUCTIONS BEFORE COMPLETING FORM

1. REPORT NUMBER (18) AFRPL-TR-79-14 ✓	2. GOVT ACCESSION NO.
3. RECIPIENT'S CATALOG NUMBER Rept.	
4. TITLE (and Subtitle) (6) Electrode Erosion Processes in Pulsed Plasma Thrusters	5. TYPE OF REPORT & PERIOD COVERED (9) Final 15 August 1977 - 31 January 1979
	6. PERFORMING ORG. REPORT NUMBER
7. AUTHOR(s) (10) Dominic J. Palumbo, Martin Begun, William J. Guman	8. CONTRACT OR GRANT NUMBER(s) (15) F04611-77-C-0024
9. PERFORMING ORGANIZATION NAME AND ADDRESS Fairchild Republic Company Farmingdale, NY 11735	10. PROGRAM ELEMENT, PROJECT, TASK AREA & WORK UNIT NUMBERS (16) 62302F 3058 (17) JON 3058120N
11. CONTROLLING OFFICE NAME AND ADDRESS AF Rocket Propulsion Laboratory (AFSC) Director of Science and Technology Edwards AFB, CA 93523	12. REPORT DATE (11) March 1979
	13. NUMBER OF PAGES 33
14. MONITORING AGENCY NAME & ADDRESS (if different from Controlling Office) Same as Item 11 Above (12) 39p.	15. SECURITY CLASS. (of this report) UNCLASSIFIED
	15a. DECLASSIFICATION/DOWNGRADING SCHEDULE

16. DISTRIBUTION STATEMENT (of this Report)

Approved for Public Release. Distribution Unlimited

17. DISTRIBUTION STATEMENT (of the abstract entered in Block 20, if different from Report)

(14) NS-18-1R0001

18. SUPPLEMENTARY NOTES

NONE

19. KEY WORDS (Continue on reverse side if necessary and identify by block number)

Electric Propulsion
Plasma Propulsion
Space Propulsion
Electrode Erosion
Arc Discharges

20. ABSTRACT (Continue on reverse side if necessary and identify by block number)

During the course of this program it was determined that material melting is the primary physical phenomenon leading to erosion of the anode electrode. Experimentation with various materials indicated that minimum erosion of the anode was obtainable using Poco Graphite but significant impulse bit reduction due to the high resistivity of this material would be incurred if this material were used. The material yielding the next least amount of anode erosion was shown to be copper (OHFC).

DD FORM 1 JAN 73 1473

UNCLASSIFIED

SECURITY CLASSIFICATION OF THIS PAGE (When Data Entered)

408 278

Various modifications to the thruster propellant/electrode configurations were attempted using Graphite in attempting to recover the loss in thruster performance associated with the use of this material as an anode electrode. These attempts were unsuccessful, and the decision was made about midway through the program to concentrate on minimizing the effects of the arc heat load on a copper anode surface by reconfiguring the electrodes and/or propellant rods. This approach to the problem not only led to a successful solution of the anode erosion problem, but also resulted in improved thruster performance and the capability of storing sufficient propellant to meet a total impulse requirement far in excess of the program goal using the original helical rod storage system with modified propellant rod width.

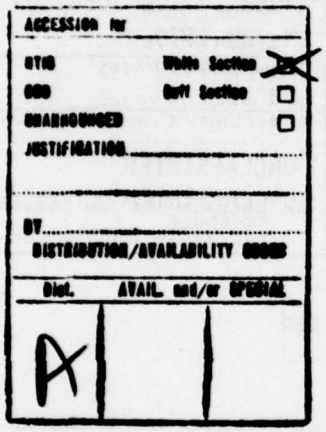

TABLE OF CONTENTS

LIST OF ILLUSTRATIONS

1.0 INTRODUCTION

A continuous long term endurance test of a one millipound pulsed plasma propulsion system was recently performed at Fairchild Republic Co. The reason for that test was to determine the factors which might lead to reduced life of such a system, and among the potential lifetime limiting phenomena detected, erosion of the anode electrode appeared to be the most critical. This program was therefore initiated with the objective of increasing the life expectancy of the anode electrode to a point beyond that required to perform a 36,000 pound-second (160,200 N-s) mission.

The specific reason for concern with regard to anode erosion on pulsed plasma thrusters stems from the solid propellant feed concept employed. Propellant rods are forced into the electrode gap by negator springs pushing from the back of the rods. The position of the rods within the electrode gap is maintained by a portion of the anode electrode called the fuel retaining shoulder (see Figure 1). Significant erosion of the retaining shoulder beginning in the vicinity of the downstream propellant section was observed during endurance testing. The conclusion reached was that eventually the downstream portion of the shoulder would be completely eroded away prior to achieving the goal for thruster system life. The total disappearance of the retaining shoulder would allow the outermost propellant sections to butt together under the action of the springs and cause system failure.

The approach used for resolution of the severe anode erosion problem was threefold. Program Phases I and II were devoted to investigation of various alternate anode materials and geometric configurations, respectively. The third phase of the program would have pursued the dependance of electrode erosion and overall thruster performance on initial discharge energy, but program review at the end of Phase II led to redirection of the effort for the continuation of Phase II in lieu of Phase III. The overall program was also supported by theoretical analysis in order to pinpoint the predominant phenomenon leading to anode erosion.

Some thirty individual tests of 100,000 discharges (or more) duration performed at FRC during this program led to solution of the anode erosion problem, increasing the life expectancy of the anode electrode in excess of the overall system design life. Moreover, as a result of solving the erosion problem, thruster specific impulse and thrust efficiency were significantly improved.

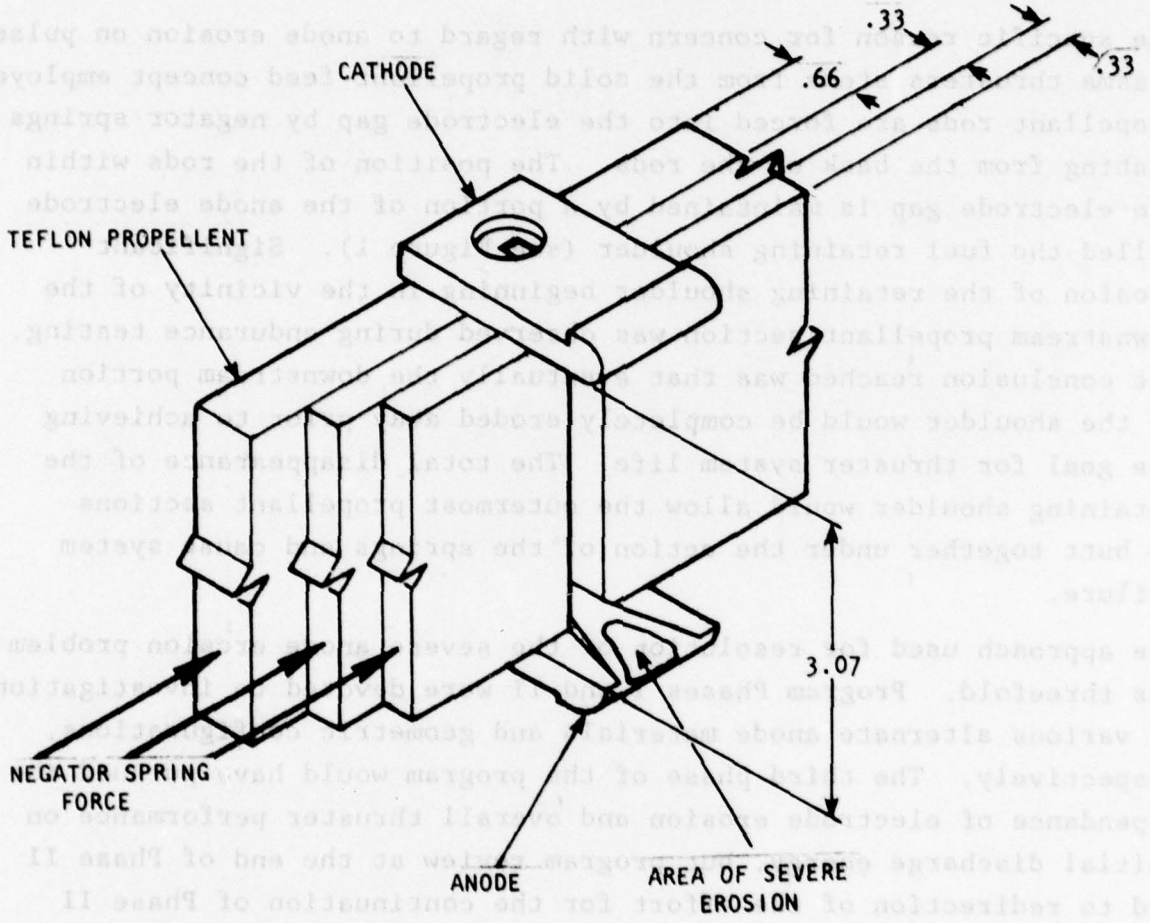

Figure 1. Illustration of Propellant Feed System

2.0 TECHNICAL APPROACH

2.1 Thruster Operational Characteristics

The one millipound pulsed plasma thruster utilizes solid polytetrafluoroethylene (PTFE) propellant, the chemical formula of which is $(-C_2F_4-)_n$. There are many manufacturers of PTFE in the US, each of which markets its product using a different brandname. The basic difference between one brand and another is the average molecular weight (or, degree of polymerization) of the homopolymer molecule chains. The particular product used at FRC as propellant for pulsed plasma thrusters is Teflon, produced by DuPont.

Figure 1 shows the general configuration of the electrode/propellant geometry generated as a result of performance goal testing during the program of Ref. 1. The interelectrode spacing is 3.07 inches (7.8 cm) and the gap between propellant rods is 0.3 inches (7.62 mm). Each of the "side fed" propellant rods is divided into three individual sections which are fed independently (using separate negator springs) in order to accommodate for the increasing propellant burn rate with downstream position. The innermost propellant section is 0.66 inches (1.68 cm) wide while the center and outermost (furthest downstream) propellant rods are each 0.33 inches (0.84 cm) wide. The burning rates from innermost to outermost propellant rods are in the proportion 0.16, 0.30, 0.54 based upon mass.

The 750J of discharge energy is stored in four capacitors, totaling 240±10% microfarads, charged to a nominal voltage of 2.5kV. Thruster discharge is initiated by firing a solid state ignitor plug into the electrode gap. A typical discharge exhibits a single damped sinusoidal characteristic with 120kA peak current and 35kHz frequency. The impulse bit after complete burn-in of the propellant rods is 5 mlb-s (22.2mN-s) at 1600s specific impulse.

The electrode erosion level being experienced at the onset of this program with copper being used for both the anode and cathode was 16.4 ug per discharge overall, about 73% of which was anode erosion. The level of cathode erosion is not considered to be significant because it is distributed fairly uniformly over a large area and poses no functional problems. The thruster life expectancy necessary to achieve the minimum required total impulse is 7.2 million pulses. This translates to 86.4 g of anode material at the above mentioned erosion rate, or, 9.7 cm^3 of electrode volume.

2.2 Possible Mechanisms for Anode Erosion

Two erosion mechanisms were evaluated throughout this program in an attempt at isolating the predominant physical phenomena leading to erosion of the anode. The mechanisms considered were:

(i) Melting and subsequent molten metal removal.

(ii) Sputtering by negative ions.

The heat input to the surface of the anode via electron bombardment was thought to be of sufficient magnitude to cause local melting. In all probability the molten material would not vaporize but rather would be swept away from the solid metal below either by viscous shear forces at the plasma/liquid metal interface or by electro-hydrodynamic (EHD) extraction of liquid droplets from the molten pool; or a combination of those phenomena. The possibility that negatively charged ion bombardment of the anode surface might cause sputtering of the electrode material was considered primarily because the decomposition of Teflon yields atomic fluorine, which has the highest affinity for electrons of all the elements.

Experiments were carried out with the objective of determining which of the phenomena cited above is the primary contributor to anode erosion in pulsed plasma thrusters. These experiments are described in subsequent sections of this report. Theoretical analyses of these two possible mechanisms is presented in the next section. These analyses were carried out with assistance from Dr. J. Perel of Phrasor Technology, subcontracted to FRC for this purpose.

2.3 Theoretical Analysis of Possible Erosion Mechanisms

2.3.1 Material Melting

A simplified analysis of material melting under the action of an external source of heat is presented in Ref. 2. The integral equations of heat transfer with time and one spatial dimension as independent variables are developed in order to solve the problem of surface melting on a semi-infinite plane. It is assumed that the temperature of the material remains fixed at its initial value as distance from the surface approaches infinity and that the material properties are independent of temperature. The heat flux to the surface is $F(t)W/cm^2$, applied at $t=0$.

The first part of the problem is to determine at what time the surface of the material reaches its melting point. One can obtain this from the general solution for surface temperature as a function of time:

$$T_s(t)=T_o+\sqrt{\frac{3}{2\rho ck}}\left[F(t)\int_o^t F\ (T)dT\right]^{\frac{1}{2}} \qquad (1)$$

Where, ρ, c, k, are the material density, heat capacity, and heat conductivity; respectively, and T_o is the initial temperature of the slab. One can conclude from this expression that for a given heat flux, the parameter ρck will determine how quickly the surface of a material will reach its melting point, if ever. This parameter is of interest since the total arc duration is only 30 microseconds, with 85% of the energy stored in the capacitors delivered in the first 10 microseconds. If a material is to begin melting within that time period, the surface temperature must reach the melting point during that period of time. Rearranging eq. (1) with $T_s(t_m)=T_m$=material melting point one obtains.

$$\left[F(t_m)\int_o^{t_m} F(T)\,dT\right]^{\frac{1}{2}} = \sqrt{\frac{2\rho ck}{3}}\ (T_m-T_o) \qquad (2)$$

The parameter $T_m\sqrt{\rho ck}$ is presented in Table 1 for various materials of interest. Physical constants were obtained from Ref. 3.

TABLE 1. THE PARAMETER $T_m\sqrt{\rho ck}$ FOR VARIOUS MATERIALS

Material	$T_m\sqrt{\rho ck}$ (W/cm^2)
Tungsten	6535
Molyblenium	4754
Graphite	4436
Tantalum	4072
Copper	3912
Platinum	2869
Thorium	1405

If F(t) is assumed constant and one asks what level of heat flux is required to bring the materials in Table 1 to their melting point in 10 microseconds, it is found that for heat flux between 0.44 and 2.06 MW/cm^2 all of the materials listed will reach their melting points in that time. In order to bring the tabulated materials to their melting points in one microsecond, flux levels between 1.4 and 6.5 MW/cm^2, depending upon the material, would be required.

Order of magnitude calculations based upon estimated values of the current density and anode fall potential indicate that heat flux of the form $\bar{J}\cdot\bar{E}$ at the anode surface can easily be as high as 4 MW/cm^2. An independent estimate of the average total heat power into the anode was obtained via calorimetric measurement of the total energy dissipated in the anode. Roughly 8% of the total 750J is input to a copper anode during the 30 μs discharge. Taking 85% of this over the first 10 μs of the discharge leads to an average heat flux of 5MW during that time period. The conclusion reached on the basis of these calculations is that there is sufficient heat flux at the anode surface for sufficient time to cause any of the materials listed in Table 1 to reach their melting point. The next question is whether or not there is sufficient time to actually cause melting. Analysis of this problem is somewhat more complicated due to the presence of solid/liquid and liquid/gas interfaces. Some simplification is possible with the assumption that the liquid is completely removed instantaneously upon its appearance. Such an assumption is typically made in reentry ablation calculations and can be considered valid in the problem at hand not only because of the high speed gas flow adjacent to the surface but also because electrohydrodynamic forces on the liquid surface can be large enough to extract liquid droplets (4).

Instantaneous and complete removal of the molten metal leads to a single interface at the solid surface. The temperature at the surface is held constant at the melting point of the material and the second boundary condition at the surface is obtained via an energy balance. That is, the total heat flux at any instant is equal to the sum of the heat conducted away from the surface per unit area ($-k\partial T/\partial x$) and the heat of fusion necessary to melt a unit volume of material. The location of the surface with respect to its original (premelt) location is one of the variables and the heat penetration depth (i.e., point at which $T=T_o$) is the other. The differential equations can be solved directly only in the case of constant heat flux. Numerical solution is required for solution in problems wherein the heat flux is time variant.

Calculations were performed in which the heat flux was assumed to have the form

$$F(t)=F_{max}e^{-\alpha t}\sin\omega t \qquad (3)$$

where α and ω were obtained from discharge current oscillographs and F_{max} was varied to determine how much material would melt during the first half-cycle of the discharge as a function of F_{max}. Calculations begin at $t=0$ with $T=T_o$ everywhere in the material. Eq. (2) is solved for the time at which $T_s = T_m$ and beyond that point the material melting problem is solved up to $t=\pi/\omega$.

Maximum flux levels of from 1 to 10MW/cm^2 were assumed and calculations indicated that for heat flux on the order of 4MW/cm^2 the total mass melted per unit area would be within the range of values expected on the basis of measured erosion rates for all materials considered. The order of materials from least to most melt per unit area under the same conditions was computed to be graphite, molylybdenum, tungsten, copper, tantalum, and platinum. Graphite came out significantly better than any of the metals considered because of its relatively high heat of sublimation (graphite changes directly into a gas at 3300^{o}C) by comparison to the heats of fusion typical of the metals.

It was concluded that melting is certainly a possible mechanism for anode erosion at the levels being experienced at the onset of this program using copper and that the prognosis for improvement by changing the anode material to one of the better materials was good.

2.3.2 Material Sputtering

Calculation of the sputtering yield by an arbitrary ion bombarding an arbitrary surface material is not generally possible to do. The reason for this is the lack of a sufficiently general theoretical formulation of the sputtering process. Not only is the yield dependent upon the target material and bombarding ion but there is also strong dependence on the energy of the bombarding ion and angle at which the ion strikes the target's surface. The energy distribution function of the bombarding ions is also an important variable since the probability of sputtering atoms of target material is related to the number of ions striking the surface which have sufficient energy to release the target atoms. Detailed calculations were therefore

not performed, but estimates have been made which are based upon the experimental data presented in Ref. 5.

The energy in electron volts (eV) which a singly charged ion will possess after falling from rest through a potential is numerically equal to the potential. A reasonable estimate of the average potential across the electrode gap during the first half cycle of the discharge was obtained from the current and voltage oscillographs. A value of 200-300V was estimated, leading to a maximum ion energy of 200-300eV.

A "ballpark" estimate of the sputtering yield which one would expect from 300 eV negative fluorine atoms can be extracted from Ref. 5. For 400 eV ion bombardment of copper, one would expect a sputtering yield of between 1.5 and 2 atoms per ion, based upon experimental data generated for positive bombardment ions having roughly the same atomic number as fluorine.

Since sputtering yield varies fairly linearly below threshold energy, one can estimate that a 300 eV ion would have a yield on the low side of this range and so an estimate of 1.5 atoms/ion is chosen. The next step in this qualitative analysis is to estimate the number of negative fluorine atoms which might exist and the fraction of those which might have 400 eV of energy upon arrival at the anode. These estimates are much more difficult to make and one must rely on physical intuition, for the most part. The total number of fluorine atoms present during one discharge would be 3.6×10^{19} if the 1.5 mg of Teflon ablated were completely dissociated. In all probability, the higher energy negative fluorine ions formed would exist only during the first quarter-cycle of the discharge, during which time about 50% of the total amount of Teflon ablated would be present. Hence, it is assumed that roughly 1.8×10^{19} fluorine atoms are available for production of higher energy negative ions. Of these, it is estimated that about one tenth of one percent will become negative ions and roughly 20% of these will arrive at the anode with 400 eV of energy. Thus, the total number of F- ions striking the anode with a sputtering yield of 1.5 atoms/ion would be roughly 4×10^{16}. The atomic weight of copper is 63.5 amu, which translates to 1.05×10^{-25} kg per atom.

increased to a more respectable value. Anode area

The total amount of copper which would be sputtered, therefore, is $(1.5)(1.05\times10^{-25})(4\times10^{16})=6.32\times10^{-9}$kg, or, 6.32 ug. By comparison, the actual erosion per discharge of a copper anode is 12 μg, which is of the same order of magnitude as the sputtering estimate.

The conclusion is, therefore, that sputtering by negative fluorine ions could yield erosion at the level measured using copper. The data of Ref. 5 indicate that materials such as tungsten, molybdenum, and tantalum will have a higher resistance to sputtering than copper; i.e., the sputtering yield of ions on these materials should be about one third of that on copper. Interestingly enough, graphite should exhibit the highest resistance to sputtering of all the elements at 400 eV ion energy.

2.4 Results of Materials Testing

Testing was performed on ten different material combinations. Graphite, copper, 2% thoriated tungsten, tantalum, copper coated with 10 mils of tungsten, arc cast molybdenum, 25% copper impregnated tungsten, and platinum were all tested using a copper cathode and Teflon propellant. One test in which the cathode material was 17-7PH stainless steel and the anode material was copper, and one test using a copper anode and cathode with Celcon propellant were also performed as part of the materials testing phase. A test using copper impregnated graphite was performed during the geometry variation phase.

All tests were run for approximately 100,000 consecutive discharges on an around the clock basis (i.e., 7 days of continuous running). Thruster impulse bit measurements were made daily and overall average impulse bit was computed by numerically integrating impulse over number of discharges and dividing by the total number of discharges at the end of the test. Thruster specific impulse was obtained by accurately weighing the propellant rods before and after testing. Anode and cathode erosion per discharge were obtained by dividing the difference in weight of each as measured before and after testing by the total number of discharges. The results of materials testing are presented in Table 2. An engineering drawing of the anode electrode used for all materials testing is shown in Figure 2.

TABLE 2. RESULTS OF MATERIALS TESTING

ANODE MATERIAL	NUMBER OF DISCHARGES	I_{AVE} (MLB-S)	$I_{SP(S)}$	ANODE EROSION PER DISCHG (ug)	CATHODE EROSION PER DISCHG (ug)	ANODE EROSION PER TOTAL IMPULSE (MG/LB-S)
COPPER	103,508	5.42	1660	11.99	4.36	2.214
GRAPHITE	101,452	4.53	2180	4.59	3.17	1.012
THORIATED TUNGSTEN	98,148	5.23	1820	40.25	4.10	7.694
TANTALUM	101,800	5.36	1800	27.72	1.76	5.171
COPPER/SS CATHODE	99,066	5.08	1740	15.38	11.16	3.029
TUNGSTEN COATED COPPER (10 MIL)	101,489	5.39	1810	15.16	1.55	2.812
ARC CAST MOLYBDENUM	100,207	5.37	1780	16.93	3.48	3.158
25% COPPER 75% TUNGSTEN	100,953	5.40	1750	27.81	3.86	5.155
PLATINUM	95,222	5.36	1500	22.79	1.18	4.252
COPPER CELCON PROPELLANT	58,646	-	-	27.79	-	-

NOTE: ALL TESTS

COPPER CATHODE, 1.3" WIDE PROPELLANT (0.66, 0.33, 0.33)
BASIC ANODE AND CATHODE GEOMETRY

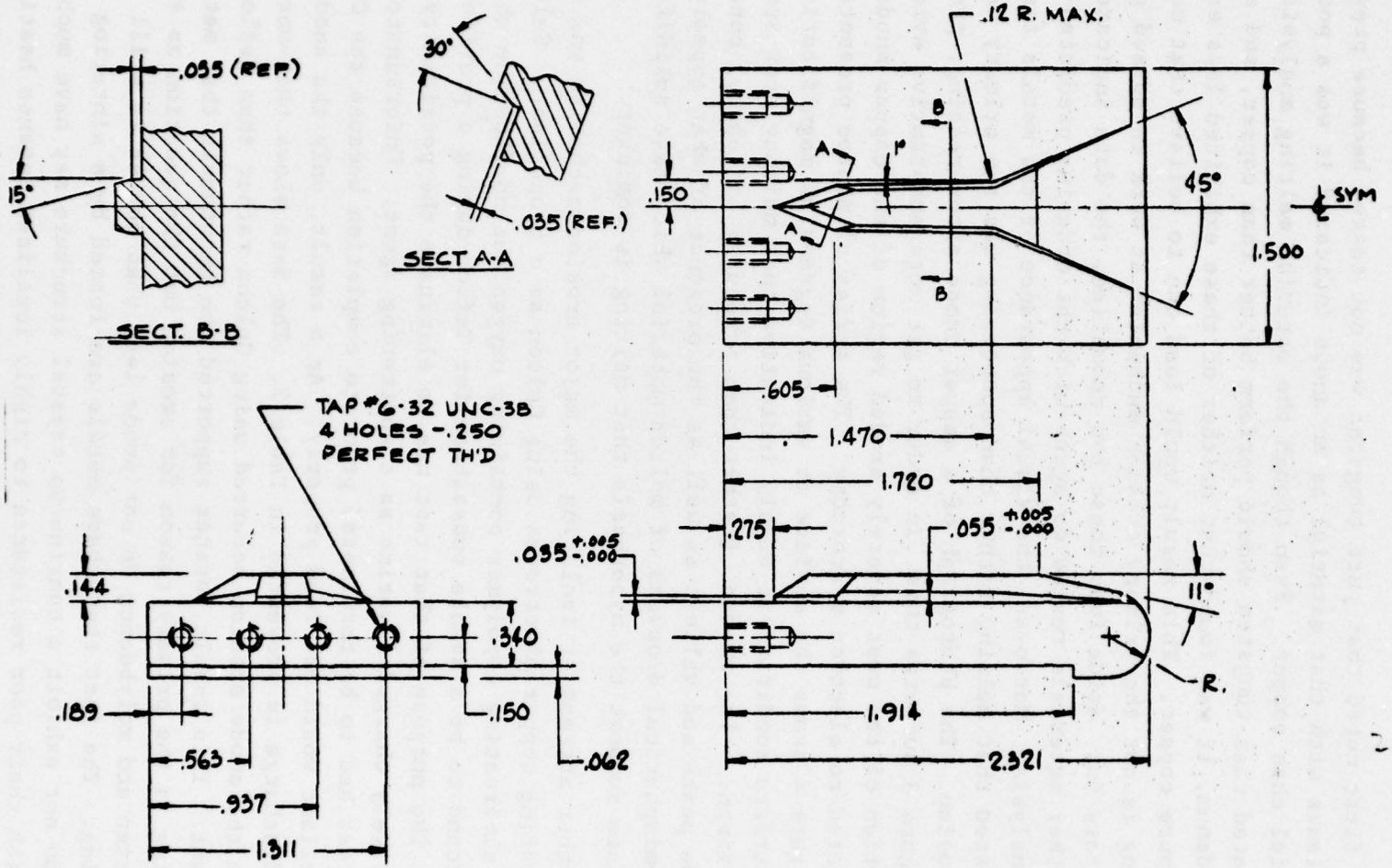

Figure 2. Basic Anode Configuration

It is first noted that pure tungsten was not tested because previous experience with that material as an anode indicated it was a poorer material than copper. Even though the material melting analysis indicated that tungsten should perform better than copper, and so should molybdenum, it was found that neither of these exhibited less erosion than pure copper. This result would lead one to believe that material melting is not the primary erosion mechanism at work in pulsed plasma thrusters but, aside from these two anomalies, the data indicate that all other materials tested do agree with the ordering predicted by the analysis. Moreover, the visual appearance of the metals tested suggested that melting rather than sputtering was the primary cause of erosion. The photograph of a copper anode after testing, presented in Figure 3, supports this. In order to get more substantive evidence, a section of the most severely eroded region of the copper anode was subjected to electron microscopy. The series of photos presented in Figure 4 shows the surface at various degrees of magnification. The surface condition is highly indicative that melting, not sputtering, is dominant. The smooth, (rather than irregular and sharp) condition of the peaks and valleys as well as the presence of what appears to be hemispherical droplets of molten material which have solidified in place support the hypothesis that melting is dominant.

A further attempt at isolating the major erosion mechanism was made by testing copper electrodes using Celcon as a propellant. Celcon is a alternating copolymer containing oxygen but no fluorine which was found to be a usable substitute for Teflon during a previous program (6). The purpose of that test was to eliminate the possibility of negatively charged fluorine as a sputtering agent. Unfortunately, the test had to be terminated prior to completion because the Celcon propellant would not feed properly. As a result, only the anode erosion per discharge is presented in Table 2. The data shows that more than twice the anode erosion occurred using Celcon rather than Teflon propellant. This result further supported the hypothesis that material melting is the primary reason for erosion but the question as to why tungsten and molybdenum do not erode less than copper is still perplexing. The fact that these metals are formed by a sintering process and do not exhibit a continuous crystal structure may have much to do with their poor resistance to highly localized intense heating. The question was addressed to some extent by testing arc cast

Figure 3. Photograph of Copper Anode After Testing

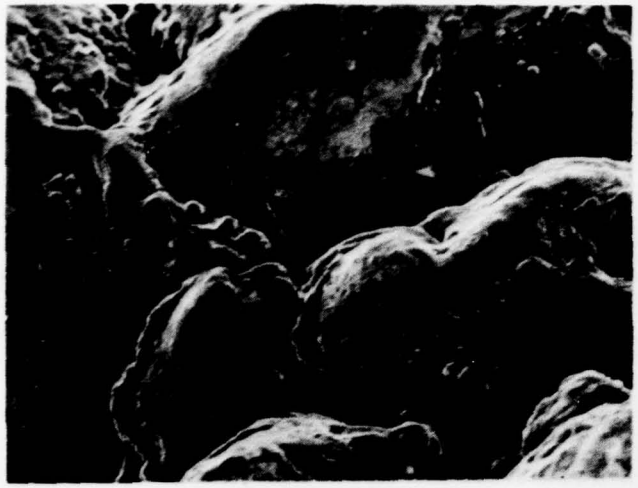

A - 220 X

B - 550 X

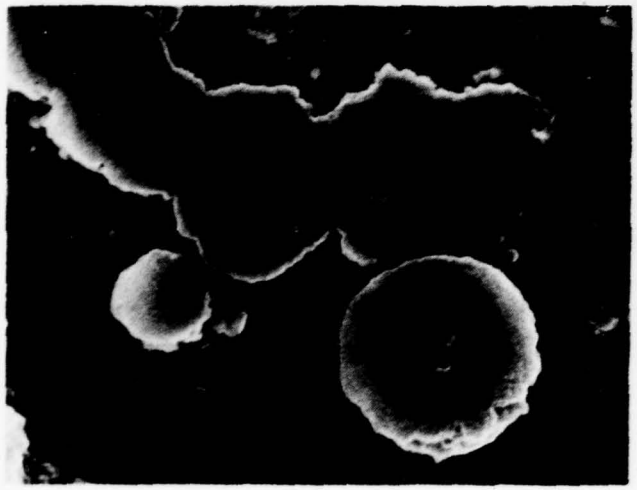

C - 2200 X

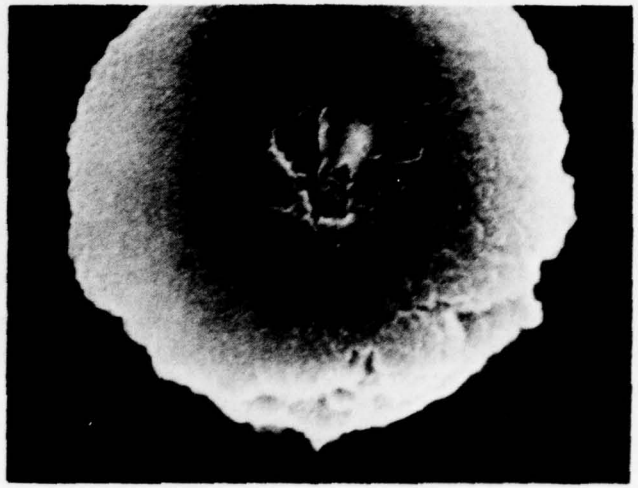

D - 5400 X

Figure 4. Electron Micrographs of Copper Anode Surface

molybdenum and copper impregnated tungsten, the objective being to provide a more homogeneous and continuous metal structure than the normal sintered metal exhibits. The data shows, however, that neither of these materials erodes less than pure copper.

The most erosion resistant material of all those tested turns out to be graphite. The particular graphite used for testing was obtained from Poco Graphite and is their grade DFP-3-2. Although graphite erodes only about one third as much as copper, which is next best, a significant decrease in impulse bit (about 16%) was measured. The decreased impulse bit, probably a result of the high resistivity of graphite as opposed to copper, led to decreased total impulse for a comparable number of discharges. Hence, anode erosion per total impulse was only reduced by a factor of 2. This was still considered to be a great improvement over the copper but other factors had to be considered before making a final decision as to which material was indeed "best". Reduced impulse bit would require longer capacitor life because a larger number of discharges would be required to deliver a given total impulse. Furthermore, an additional 36W of power would be required in order to generate one millipound of thrust. One advantage associated with using graphite, in addition to reduced erosion, would be a savings of 5.4 pounds (11.9 kg) of propellant mass due to the higher specific impulse. As a result of these trade-offs the decision regarding the final choice of electrode material was not made prior to initiating Phase II testing. It was decided that geometric changes to the electrode shape and/or propellant configuration would yield further insight and allow for a more enlightened decision.

2.5 Results of Configuration Changes

The first modification to the original propellant/electrode geometry was to redistribute the thickness of the three propellant sections within the 1.32" (3.3 cm) width. The original design incorporated an innermost (upstream) rod 0.66" (1.68 cm) wide and two outer sections each 0.33" (.84 cm) wide. This placed the outermost rod against the retaining shoulder beginning at a distance of 0.99" (2.51 cm) downstream. Redistribution of the rods into equal width sections of 0.44" (1.12 cm) width would put the outermost rod a

distance 0.88" (2.24 cm) downstream, allowing an additional 0.11" (2.8 mm) of shoulder ahead of the rod. The results of testing this new propellant rod distribution, as well as the original for comparison, are presented in the first two lines of Table 3. Note that about 56% more erosion was measured with the new propellant rod configuration than with the original while thruster performance showed a slight increase. It did appear that the cut-off point for severe erosion was further downstream than the furthest upstream position of the outermost rod, and that as a result the ability of the retaining shoulder to maintain the position of this rod would yield a larger total impulse capability prior to failure in spite of the higher rate of erosion. Best estimates indicated however, that the 36,000 pound second requirement would not be met.

The next two modifications were inspired by the results of materials testing, wherein it was found that Poco Graphite is the most erosion resistant material of all those tested. The decreased impulse bit associated with the use of graphite as the anode material makes this material undesirable from an overall system viewpoint, however, and the two configurations described next evolved with the intention of increasing the impulse bit with a graphite anode.

A composite anode was designed in which the shoulder portion was fabricated from Poco Graphite and the downstream portion from copper. An engineering drawing of that electrode is presented in Figure 5. Note that the downstream copper portion of the electrode is connected, via a continuous copper path, directly to the strip lines. This allows the discharge current to bypass the graphite portion of the electrode once the arc current begins flowing through the electrode end. The intention of this design was to force the bulk of the discharge current to flow through the highly conductive copper portion while maintaining the excellent erosion resistance of graphite in the critical retaining shoulder region. Test results are presented on the third line of Table 3. The 4.59 μg of anode erosion is the sum of the copper and graphite portions. It is observed that there is only a

TABLE 3. RESULTS OF GEOMETRY STUDIES

GEOMETRY	ANODE MATERIAL	$I_{AVE.}$ (MLB-S)	I_{SP} (S)	ANODE EROSION PER SHOT (ug)	CATHODE EROSION PER SHOT (ug)	ANODE EROSION PER TOT. IMP. (MG/LB-S)
BASIC (.66, .33, .33)	COPPER	5.42	1660	11.99	4.36	2.214
BASIC (.44, .44, .44)	COPPER	5.60	1780	18.80	1.16	3.354
BASIC (.66, .33, .33)	COMPOSITE COPPER/ GRAPHITE	4.61	2180	4.35	-	0.943
WIDE FUEL (.58, .58, .58)	COPPER	5.62	1650	11.94	1.18	2.126
WIDE FUEL (.58, .58, .58)	GRAPHITE	5.10	1570	6.84	-	1.340
WIDE FUEL (.58, .58, .58)	COPPER FILLED GRAPHITE	5.03	1810	7.60	0.90	1.509
FLARED (.66, .33, .33)	COPPER	5.32	1890	7.89	3.80	1.482
FLARED 600 JOULES	COPPER	4.47	2000	3.64	1.73	0.814
LONG WIDE FUEL	COPPER	5.32	2270	0.76	0.52	0.144

NOTE: ALL TESTS

COPPER CATHODE

MINIMUM OF 100,000 PULSES

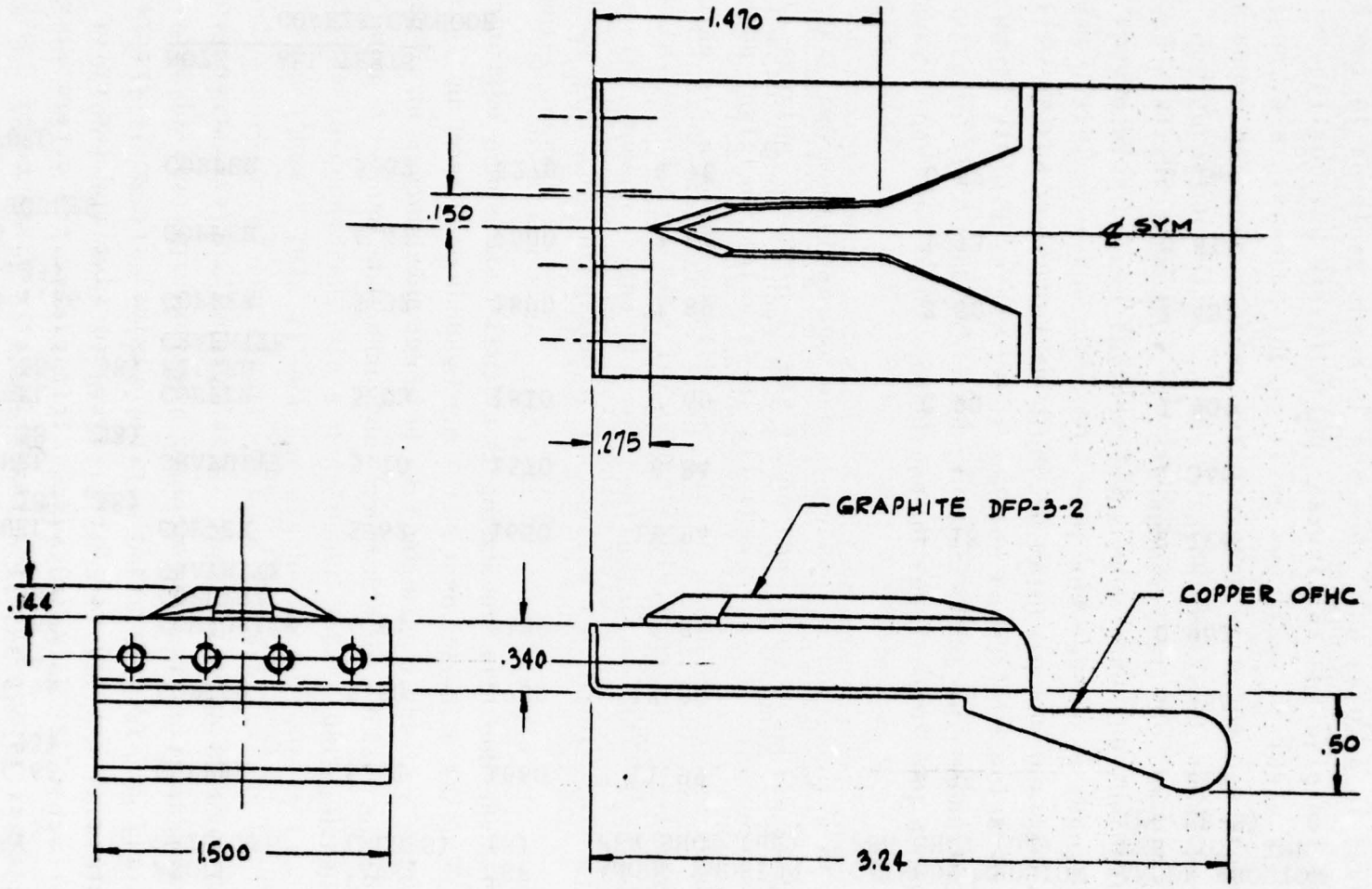

Figure 5. Composite Copper/Graphite Anode

slight difference between these results and the results obtained using a pure graphite electrode. It was observed that the graphite portion was most severely eroded at the interface seam between it and the copper portion. This type of phenomenon has been observed before where an interface between ceramic insulation and conductive material is exposed to the arc. The arc will aways have a tendency to severely erode both at the interface. Graphite is not an insulator, but the conductivity is three orders of magnitude lower than that of copper and this apparently leads to the same kind of erosion pattern as with the noted insulator/conductor interface.

The second attempt at increasing impulse bit using a graphite anode was the result of experience gained in previous experimentation designed to parametrically determine the dependence of thruster performance on propellant/electrode configuration (7). It was demonstrated that the amount of propellant surface area exposed to the discharge has a direct effect upon the amount of mass ablated in a given propellant configuration, and that the effect of introducing more propellant mass into the discharge at a given discharge energy was to increase the impulse bit and decrease the specific impulse with slight reduction of thrust efficiency. It was reasoned, therefore, that widening the propellant rods to supply more mass to the discharge should increase the impulse bit obtained using a graphite anode and lower the specific impulse. A series of calculations were made using the empirical correlations presented in Ref. 7.to determine just how much of an increase in area would yield performance comparable to that obtained using copper. It was concluded that a 35% increase in the width of the propellant rods would be appropriate. The original propellant width of 1.3" (3.3 cm) was therefore increased to 1.75" (4.45 cm), resulting in an increase from 7.8 in^2 (50.3 cm^2) to 10.5 in^2 (67.7 cm^2) of exposed propellant surface area. The new propellant rod sections were of equal 0.584" (1.48 cm) thickness.

A test was first run to determine the baseline performance of a set of copper electrodes using the new propellant width. The newly designed electrodes were lengthened to accommodate the larger width of propellant and an engineering drawing of this new design is presented in Figure 6. Results of running the copper and Poco Graphite electrodes using the wide fuel configuration are presented on the fourth and fifth lines of Table 3. Note that the impulse bit achieved using the wider propellant and graphite anode did increase by about 13% over that obtained using the original design but was still 10% lower than that achieved using a copper anode in the same configuration.

Moreover, a much more severe decrease in specific impulse was measured than anticipated (i.e., from 2180s to 1570s). This probably occurred because the increased length of the current path through the graphite led to a nonnegligible increase in overall discharge path resistance. One must realize that the entire equivalent circuit resistance of the discharge path, including the arc, is only about 30 milliohms in this thruster when copper electrodes are used. Hence, a change of only a few milliohms is a significant fraction of the total and, as such, will have a substantial effect upon the level of discharge current generated at a given discharge energy. One other observation concerning these two tests is that the erosion of the copper anode showed negligible change while the graphite eroded about 50% more in the wide fuel configuration.

During the course of running the aforementioned tests with the wide propellant rods information was received from Poco Graphite concerning a grade of graphite which, when filled with copper, had a much improved conductivity over the graphite alone. It was decided that this material should be tested and an electrode was manufactured in the configuration shown in Figure 6 to be run with the wide propellant rods, since the thruster was already set up for these rods. The data on line 6 of Table 3 show the results of that test. Impulse bit was only slightly lower but specific impulse

to release the target atoms. Detailed calculations were therefore

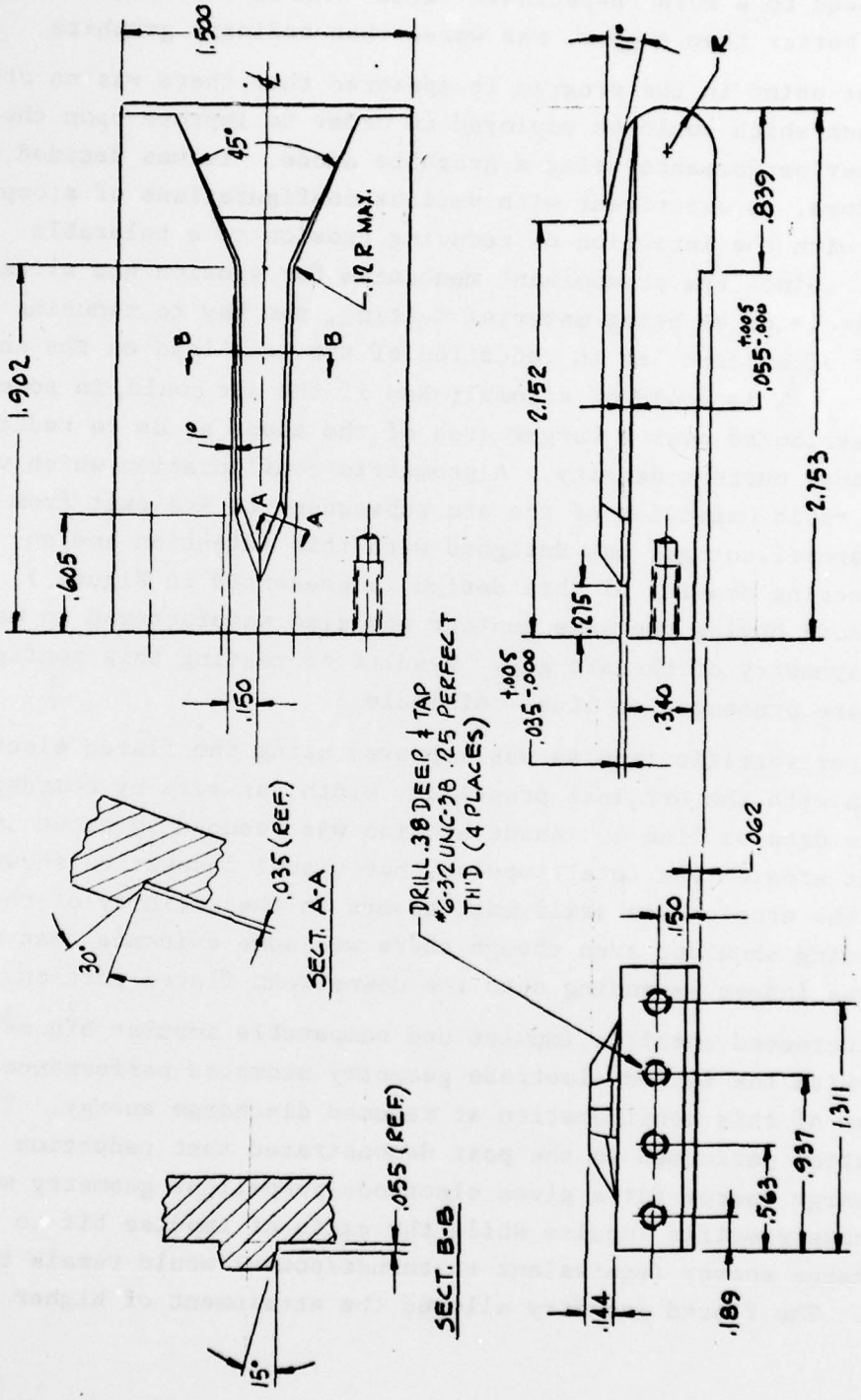

Figure 6. Anode Configuration for Wide Propellant Rods

increased to a more respectable value. Anode erosion, although still better than copper, was worse than ordinary graphite.

At that point in the program it appeared that there was no other approach which could be employed in order to improve upon the thruster performance using a graphite anode. It was decided, therefore, to experiment with various configurations of a copper anode with the intention of reducing erosion to a tolerable level. Since the predominant mechanism for erosion had already been isolated as being material melting, the key to reducing the amount of erosion lay in reduction of the heat load on the anode surface. This could be accomplished if the arc could, in some way, be distributed over a larger area of the anode so as to reduce the local current density. A geometric configuration which would cause rapid expansion of the arc subsequent to its exit from the interpropellant gap was designed with this intention and an engineering drawing of this design is presented in Figure 7. A cathode having the same contour was also manufactured to maintain symmetry of the arc gap. Results of testing this configuration are presented on line 7 of Table 3.

Thruster specific impulse was improved using the flared electrode design with the original propellant width, as seen by comparison to the data on line 1. Anode erosion was reduced by about 34%, as was erosion per total impulse, but visual inspection showed that the erosion was still most severe in the vicinity of the retaining shoulder even though there was some evidence that the arc was indeed expanding onto the downstream flared portion.

The increased specific impulse and comparable impulse bit associated with the flared electrode geometry prompted performance of a test of this configuration at reduced discharge energy. Experimentation performed in the past demonstrated that reduction of discharge energy for a given electrode/propellant geometry would decrease specific impulse while the ratio of impulse bit to discharge energy (equivalent to thrust/power) would remain the same. The flared geometry allowed the attainment of higher specific

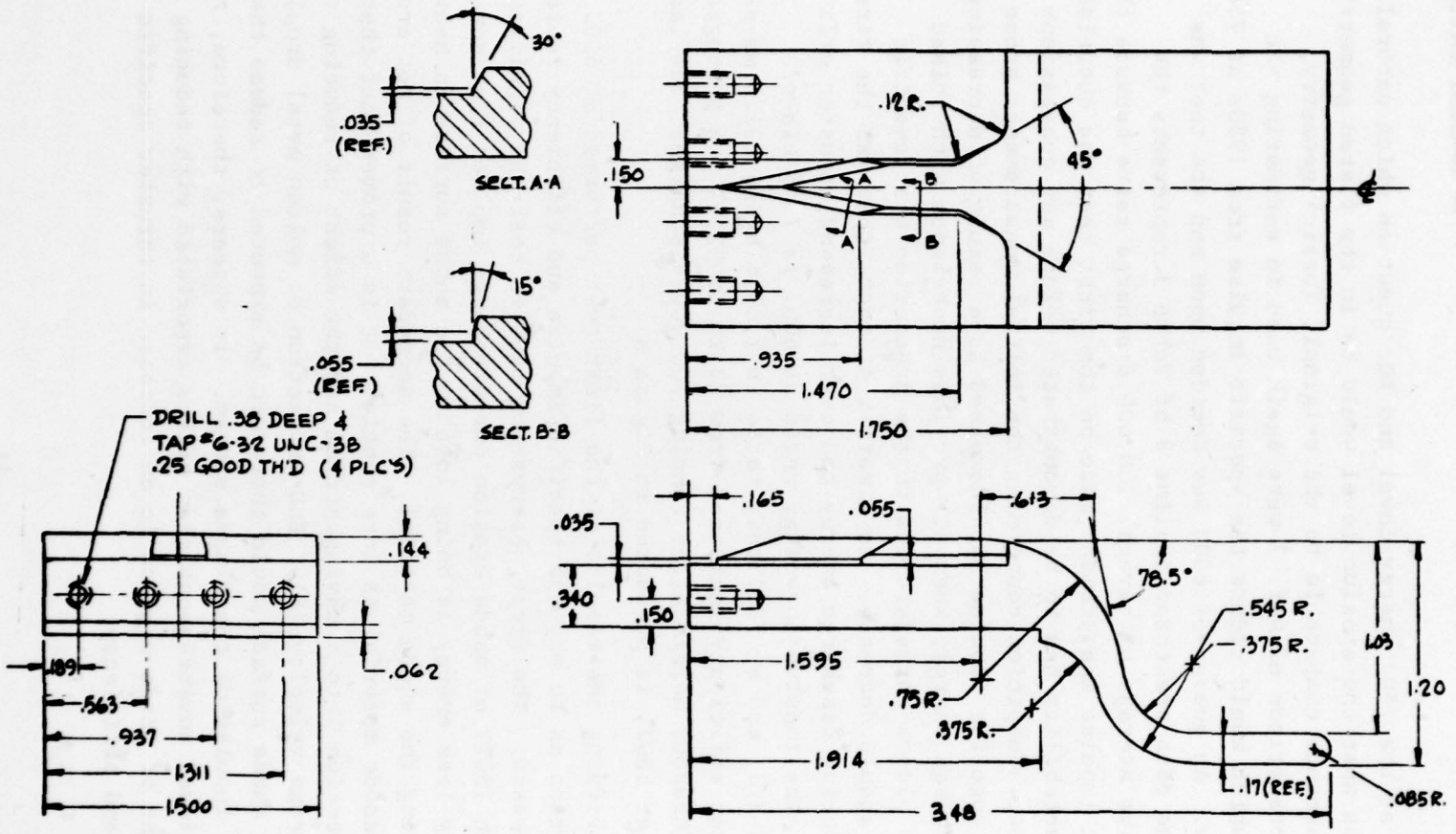

Figure 7. Flared Anode Geometry

impulse at the 750J energy level and the question which naturally arose was what the erosion level would be in the flared geometry at performance comparable to the original, (basic) geometry. Data correlations of Ref. 7 were again used in estimating the energy which would reduce the specific impulse from 1980s at 750J to 1660s. An energy of 600J was decided upon and the test was run. The data presented on line 8 of Table 3 represents the cumulative average of several 100,000 discharge tests because the specific impulse measurement made on the first test was questioned and repeatability had to be demonstrated before any conclusions were made. Suspicion concerning the initial measurements arose because specific impulse had increased as a result of decreasing the discharge energy, when all previous experience with pulsed ablative plasma thrusters led to the prediction that specific impulse should decrease. As a matter of fact, this was the first time reducing discharge energy had ever increased thruster efficiency. The impulse to energy ratio at 600J is 7.45 mlb-s/J (33.2 mN-s/J) and at 750J this ratio is 7.09 mlb-s/J (31.6 mN-s/J) and thrust efficiency increased from 29.2% to 32.5%. A photograph of the thruster nozzle after running 700,000 discharges, the last 540,000 at 600J, is presented in Figure 8.

After verifying the results of the first test performed at 600J the question as to why the specific impulse and efficiency increased was addressed. The first observation made is that the significant reduction (54%) of anode erosion per discharge implies that considerably less energy is being lost to the anode surface in heating and melting the anode material. The secondary result of not eroding as much anode material is more subtle. It is a proven fact that mass injection into a moving stream has the effect of reducing the mass average velocity (8). EHD extraction of molten metal droplets from the anode surface would therefore be expected to reduce the specific impulse of the plasma stream. It appears, therefore, that an additional advantageous side effect associated with reducing the amount of anode erosion is an increase in thruster specific impulse and efficiency.

Figure 8. Photograph of Flared Electrodes After Testing

A second approach to reducing the effect of the high heat flux at the anode surface was inspired by some of the quantitative results obtained from the heat transfer analysis described in Section 2.2.1. Although accurate numerical agreement between computed and experimental results was not obtained, certain trends became obvious from the analysis when the dependent variables were changed. One such trend demonstrated that a given material would erode far less under the action of a given heat flux if the time of application of the heat were shortened. This result is certainly obvious from a qualitative point of view, but the analysis demonstrated that material erosion increases fairly linearly with heat flux, while increasing as the square of the application time. The much stronger dependence on time of application suggest that instead of striving to decrease the local heat flux, more could be gained by reducing the residence time of the arc at any location on the anode surface. The analysis also demonstrated that as long as the flux is increasing with time at a given location the rate of melting also increases, but as soon as flux levels off and begins to decrease with time the rate of melting drops off very quickly. These two facts, together with the hypothesis that the heat flux due to the arc follows the same temporal variation as the discharge current, and the fact that the arc is indeed moving very quickly over the anode surface (until it reaches the end), led to the design of an electrode which would be long enough to keep the arc accelerating over the period of time through which the discharge current was still increasing (i.e.,over the first quarter-cycle). The discharge current peaks at about 7.5 μs and begins to fall off rapidly at 8.5 μs. For an arc moving at a rate of roughly 2 cm/μs, therefore, a distance of 17 cm would be traversed if the electrode were long enough. (By comparison, all materials testing was performed using an electrode 6.9 cm long.) Thus, the electrode length would have to be increased by more than a factor of 2 in order to keep the arc moving while the heat flux was still climbing. An electrode having a length of 6.8" (17.3 cm) was designed, the additional length being provided for insulation and fastening hardware. An

engineering drawing of this electrode is presented in Figure 9. The wide propellant configuration was chosen for testing because the results which were obtained using this propellant as opposed to the original indicated that a higher average impulse bit was possible with no sacrifice of specific impulse (cf. Table 3, the first and fourth lines).

The results of running this "long" electrode are presented on the bottom line of Table 3. Erosion was reduced by a factor of more than fifteen over the same propellant distribution with a shorter electrode (see line 4). Impulse bit decreased somewhat but specific impulse was improved by a margin of almost 38%, leading to an increase in thrust efficiency of more than 9%! The amount of anode erosion per total impulse had been decreased by almost 200% since the onset of this program. Most importantly, the level of erosion experienced using the long electrode would be acceptable; leading to the ability to perform the required mission.

A formal program review was held at the AFRPL after completing Phase II and the relative merits of proceeding with Phase III were discussed. It was decided that rather than performing energy variation tests on the long electrode/wide fuel configuration it would be more beneficial to freeze this geometry and run several tests to determine whether or not the electrode length could be shortened somewhat without sacrificing performance or increasing erosion. After these tests the best length would then be used in manufacturing an electrode which would be lightened by hollowing, similar to what would be done on a "flight" hardware version. The lightened electrode would then be tested for verification of the previous results. These changes to the program Statement of Work were incorporated at no increase in scope since no additional effort would be required to perform these tasks in lieu of Phase III testing.

The electrode length was first decreased from 6.8" (17.3 cm) to 5.8" (14.7 cm) in order to further investigate the effects of electrode length. A second test using a length of 4.8" (12.2 cm) was also planned. The results of testing the 5.8" long electrode are presented in Table 4, together with the results at 2.75" and 6.8" for comparison.

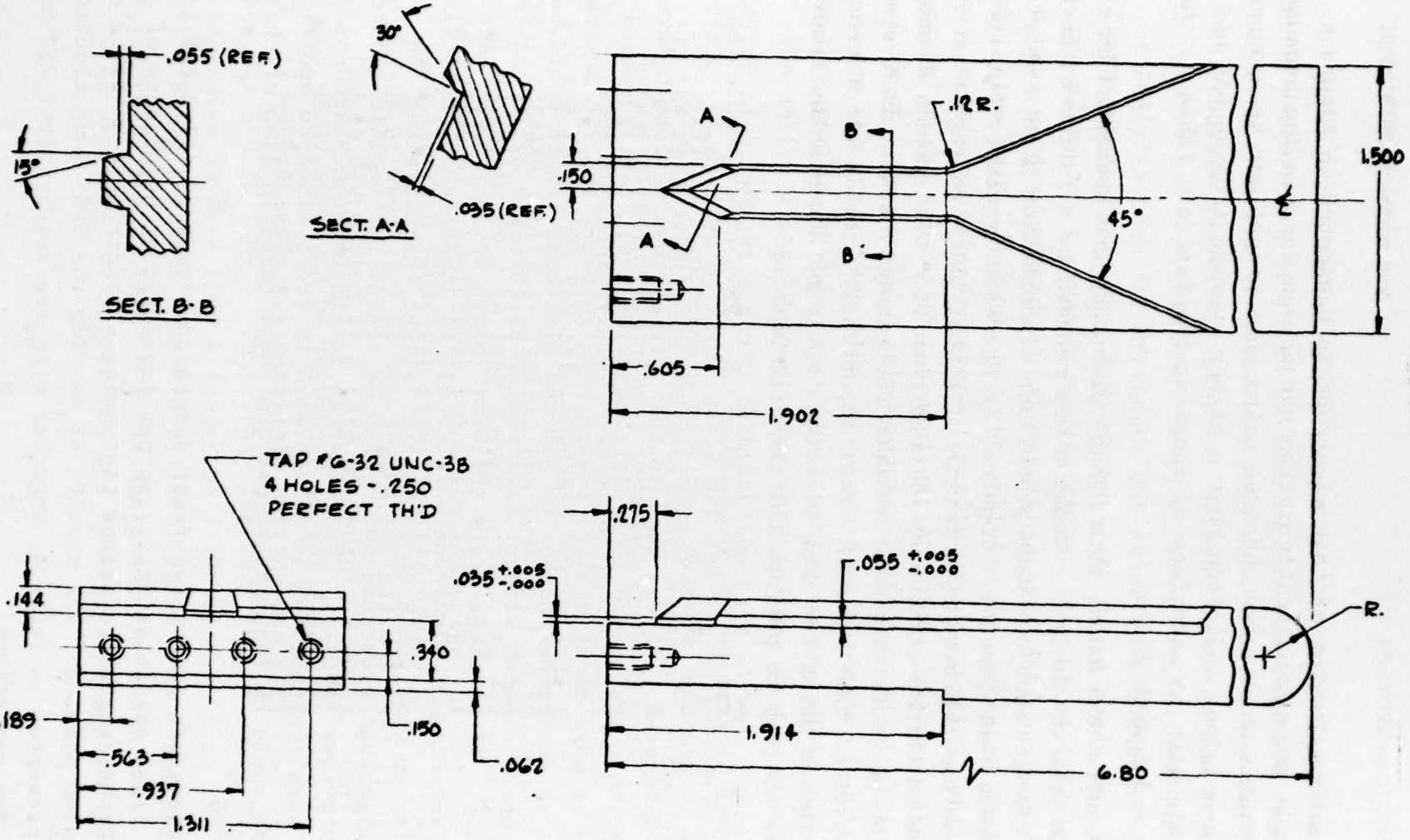

Figure 9. Long Anode Geometry

TABLE 4. RESULTS OF VARYING ELECTRODE LENGTH IN WIDE FUEL GEOMETRY

Length in (cm)	I_{AVE} (mlb-s)	I_{sp} (s)	Anode Erosion per shot (μg)	Anode Erosion per Tot. Imp. (MG/LB-S)
2.75 (7.0)	5.62	1650	11.94	2.126
5.80 (14.7)	5.63	1890	1.88	0.736
6.80 (17.3)	5.32	2270	0.76	0.144

The data shows a trend toward lower specific impulse and increased anode erosion as the electrode length is decreased. The test using the 4.8" electrode was terminated due to facilities malfunction about half way through. One would expect that the results would not have been favorable, based on the data of Table 4.

An anode having precisely the same dimensions as that shown in Figure 9 was fabricated in a lightweight configuration, similar to that which would be used on a flight system. The original (basic) copper electrode used with the wide fuel weighed 230 grams while the 6.8 inch long version weighed 710 grams. The lightened 6.8 inch electrode weighed 286g (about one third as much as the solid version). A test was run for 102,000 pulses using the lightened electrode in order to verify the previous results obtained with the solid version. Results of that test were as follows:

Specific Impulse = 2180 seconds
Average Impulse Bit = 5.66 mlb-sec
Anode Erosion per Dischg = 0.182 μg
Anode Erosion per Total Impulse = .032 mg/lb-sec

These results show that the lightened version yields essentially the same performance and is at least as erosion resistant as the original solid version. The above data also confirm the results of the two tests performed using the solid configuration and provide a sound basis for future design.

3.0 CONCLUSIONS AND RECOMMENDATIONS

Prior to initiating this program erosion of the anode on a milli-pound pulsed plasma thruster was so severe as to limit the total impulse capability of the system to approximately 5,000 pound seconds (22,250 N-S). Moreover, the original helical propellant storage and feed system would be suitable for attainment of only 28,000 pound seconds (124,600 N-S) of total impulse.

During the course of this program it was determined that material melting is the primary physical phenomenon leading to erosion of the anode electrode. Experimentation with various materials indicated that minimum erosion of the anode was obtainable using Poco Graphite but significant impulse bit reduction due to the high resistivity of this material would be incurred if this material were used. The material yielding the next least amount of anode erosion was shown to be copper (OHFC).

Various modifications to the thruster propellant/electrode configurations were attempted using graphite in attempting to recover the loss in thruster performance associated with the use of this material as an anode electrode. These attempts were unsuccessful, and the decision was made about midway through the program to concentrate on minimizing the effects of the arc heat load on a copper anode surface by reconfiguring the electrodes and/or propellant rods. This approach to the problem not only led to a successful solution of the anode erosion problem, but also resulted in improved thruster performance and the capability of storing sufficient propellant to meet a total impulse requirement far in excess of the program goal using the original helical rod storage system with modified propellant rod width.

The major achievements of this program, from a quantitative viewpoint, are:

(i) Anode erosion was reduced by 94%

(ii) Thruster Specific Impulse was increased by 36%

(iii) Thruster efficiency was increased from 26.2% to 35.1%

The impact upon the existing thruster design is summarized as follows:

(i) Propellant rod width was increased from 1.3" (3.3 cm) to 1.75" (4.4 cm)

(ii) Total propellant storage capability using the existing helical pitch increased from 17.5 lbs (38.6 kg) to 26.3 pounds (58 kg)

(iii) Total impulse capability using the existing helical pitch increased from 28,000 to 57,800 pound seconds (257,210 N-S)

(iv) Total impulse capability of 98,800 pound seconds (440,00 N-S) could be attained with a slight increase of helical pitch.

The above results are based upon experimental measurement of the relative propellant rod section burning rates over the initial 200,000 discharges. Data beyond the first 75,000 discharges is considered to be an accurate representation of the remainder of the thruster lifetime since beyond that point the impulse bit levels off after a slight initial decrease during propellant rod burn-in. It is recommended, however, that relative propellant rod section burning rates be measured over a longer test period (i.e., .5M to 1M discharges) so that the initial burn-in period becomes only a small fraction of the total. This would lead to a more accurate and reliable measurement for long term design purposes. Moreover, the thruster specific impulse measurement could be made more accurately if burn-in time were an insignificant fraction of total running time.

It is also to be noted that all measurements made during this program were made using a laboratory test thruster identical to the one described in Ref. 9. Commercially available Mylar/Castor oil capacitors having a very low dissipation factor were used on this thruster. It is of primary importance that thruster performance (especially specific impulse) be verified using the high energy density KF-film capacitors, currently under development by Maxwell Laboratories, prior to initiating final design of the propellant storage system. The relatively high dissipation factor associated

with this type of capacitor might have an undesirable effect upon thruster performance, resulting in having to store more propellant. The design life on these high energy density capacitors is 10^7 discharges. This implies a total impulse capability for the thruster system of 50,000 lb-s (222,500 N-S) assuming a conservative 5 mlb-s (22.3 mN-S) average impulse bit. There is, therefore, a 15% margin of safety in the present design which translates to a minimum required specific impulse of 1900s to perform a 50,000 lb-s mission.

4.0 REFERENCES

1. Palumbo, D. and Guman, W. "Pulsed Plasma Propulsion Technology", Interim Report AFRPL-TR-73-79. Air Force Rocket Propulsion Laboratory, Edwards AFB, Calif., September 1973.

2. Irvine, T.and Hartnet, J. "Advances in Heat Transfer", Volume 1, Academic Press, 1964.

3. JANNAF Thermophysical Tables.

4. Mahoney, J. and Perel, J., "Electrohydrodynamic Generation of Submicron Particles for Rapid Solidification", Conference on Rapid Solidification Processing Principles and Technology".

5. Carter, G. and Colligan, J. "Ion Bombardment of Solids", American Elsiver Pub. Co., Inc., 1968.

6. Palumbo, D. and Guman, W. "Effects of Electrode Geometry and Propellant on Pulsed Ablative Thruster Performance", AIAA Paper No. 75-409, March 1975.

7. Palumbo, D. and Guman, W. "Propellant Side Feed Short Pulsed Discharge Thruster Studies", NASA CR-112035, January 1972.

8. Kolesnikov, P. and Stolovich, N. "Mass Transfer Processes in Electrodynamic Plasma Acceleration", Sov. Phys-Tech. Phys, 15,6, Dec. 1970.

9. Guman, W. and Begun, M., "Pulsed Plasma Plume Studies", Final Report, AFRPL-TR-77-2, Air Force Rocket Propulsion Lab, Edwards AFB, Calif., March 1977.